Al-Azhar Bulletin of Science

Volume 25 | Issue 1 Article 2

6-1-2014
Section: Earth science

LITHOLOGICAL MAPPING IN THE EASTERN DESERT OF EGYPT,WADI UM GHEIG AREA, USING LANDSAT ENHANCED THEMATIC MAPPER (ETM+)

Ibrahim Abu El-Liel
Faculty of Sciences Al-Azhar University

Nehal Soliman
National Authority for Remote Sensing and Space Sciences

Mahmoud Bekhiet
Faculty of Sciences Al-Azhar University

Mohamed El-Hebiry
Faculty of Sciences Al-Azhar University

How to Cite This Article

Abu El-Liel, Ibrahim; Soliman, Nehal; Bekhiet, Mahmoud; and El-Hebiry, Mohamed (2014) "LITHOLOGICAL MAPPING IN THE EASTERN DESERT OF EGYPT,WADI UM GHEIG AREA, USING LANDSAT ENHANCED THEMATIC MAPPER (ETM+)," *Al-Azhar Bulletin of Science*: Vol. 25: Iss. 1, Article 2.
DOI: https://doi.org/10.21608/absb.2014.22608

LITHOLOGICAL MAPPING IN THE EASTERN DESERT OF EGYPT,WADI UM GHEIG AREA, USING LANDSAT ENHANCED THEMATIC MAPPER (ETM+)

Ibrahim Abu El-Liel*, Nehal M. A. Soliman, Mahmoud H. Bekhiet*, Mohamed S. El-Hebiry***

** Faculty of Sciences Al-Azhar University ** National Authority for Remote Sensing and Space Sciences*

ABSTRACT

Wadi Um Gheig area comprises a variety of Neoproterozoic rocks including serpentinites of ophiolite assemblage, metavolcanoclastics, schists, metavolcanics and metagabbro of island arc assemblage. The migmatite and gniesses represent high grade metamorphic rocks. The syntectonic fresh gabbro, as well as tonalite and granodiorite in addition to the late to post tectonic granitoids are recorded. Lithological mapping in the Wadi Um Gheig is carried out by using Landsat Thematic Mapper (ETM+) image enhancement techniques including RGB band ratios and supervised classification. In the present study new proposed band ratio (7/1, 3/1, 5/7) with the supervised classification are used and proved a good efficiency for discriminating and mapping the different rock units in the Wadi Um Gheig.

Keywords:Landsat Thematic Mapper (ETM+), Supervised Classification, Ratio Images, Egypt

INTRODUCTION

The Eastern Desert of Egypt as part of the Pan-African Arabian-Nubian Shield, is occupied by igneous and metamorphic rocks that were formed in the East African Orogen during the collision between East and West Gondwana and the closure of the Mozambique Ocean since ~600 Ma (Stern, 1994; Kusky and Matsah., 2003).

The Neoproterozoicrocks in the Eastern Desert of Egypt are divided into three tectonic domains, the Northern (NED), the Central (CED) and the Southern (SED) (Stern and Hedge, 1985). The study area is located in the central part of the Eastern Desert, covering ~455 Km2 between Latitudes 25o 32' - 25o 42' and Longitudes 34o 13' - 34o 28'. It is occupied by low to moderate topographic relief represented by G. Kadabora and southeastern part of G. El-Sibai. It is traversed by Wadi Um Gheig, Wadi Um Lasiefa, Wadi Kab Ahmed, Wadi El-Shush, Wadi Kab Mousa and Wadi Kab El-Rekab (Fig.1). The Central Eastern Desert of Egypt is almost exclusively built up of ophiolite, island arc assemblage, gneisses and migmatites, together with subordinate molasse sediments and late-tectonic volcanics and granitoid intrusives (El Ramly et al., 1993). The studied rock units have pre Pan-African and Pan-African age by many authors(e.g. El Gaby, 1983;Asran, 199;Khudeir et al, 1995; Kamal El-Din, 1993; Ragab et al, 1993 and Habib et al., 1985). Recent studies suggest the Neoproterozoic age for the investigated rocks (e.g. Ibrahim and Cosgrove, 2001; Bregar et al., 2002; Abdeen 2003;Abd El-Wahed, 2006; Fowler et al., 2007; Blasband et al., 2000 and Johnson et al., 2011).

2. Geological Setting

Field investigation and petrographic studies by the present authors (Fig. 2) show that the study area is composed of serpentinites (ophiolite), metavolcaniclastics, schists and metagabbro forming the highly deformed and accreted upper crust. The lower crustis composed of high grade metamorphic migmatite, gneissic tonalite-granodiorite and sheared granite. These two layers had been intruded bysyntec tonictonalite to granodiorite, late to post tectonic granitoids and fresh gabbro. The contact between these two layers is structure contact, where the sheared granite is situated inbetween along NS sinistral strike-slipe fault shear zone (Fig. 2).

3. Remote Sensing Application in Lithological Mapping

Lithological mapping by Landsat band rationing has been used by several authors (e.g. Abrams et al., 1983; Kaufmann, 1988; Abdelsalam and Stern, 1999; Sultan et al., 1986; Kusky and Ramadan, 2002; Frei and Jutz, 1989; Gad and Kusky, 2006; Youssef et al., 2009 and Sabins, 1999). There are some effective factors controlling the lithological mapping using remote sensing techniques; (1) the localization of increased concentration of minerals relative to

the background and (2) the characterization of mineral assemblages (Frei and Jutz, 1989). Band ratios are assumed to overcome the shadow and topography effects, though for this particular case because the ratio of reflectivity of any two bands for a given material is not a function of illumination. Another information on spectral differences could have been enhanced by this manipulation. The band ratio technique is the ratio of one band to another. It is prepared simply by dividing the digital number (DN) of each pixel in one band by the DN of another band (Drury, 1987), and the resulting new values are plotted as images. The main advantages of ratio images are used to reduce the variable effects of illumination condition, and suppressing the expression of topography (Crane, 1971). Furthermore, band ratio images are less correlated and chromatically enhanced than original ETM+ bands.

Band ratio composites have been used successfully in lithological mapping for the Arabian Nubian Shield and for other areas worldwide. Band selection for the different ratio images used is based on the spectral signature of these rocks (Fig. 3). When rationing techniques are applied, all the reasonable grouping of minerals are best discriminated by combination of ratios that include short-wavelength bands (i.e. 3/1, 4/1 or 4/2), the ratio of the long-wavelength bands (5/ 7) and a ratio of one band each from short and long wavelength band groups (e.g. 5/4 or 5/3) (Crippen, 1989).

4. Methodology

A single Landsat ETM scene (Path 174/ Row 042 dated on 2000) was used. Digital processing of the study area generated several products ranging from false-color composite images (742 in RGB), and band ratio images (7/1, 3/1, 5/7) (Fig. 4). It is proposed by the author to display more geologic information and depictp sharp contrast between lithologies for easier discrimination. In the present study, the authors applied band ratio techniques, (Sultan et al., 1986; Sabins, 1999 and Gad and Kusky, 2006). Moreover, the supervised classification technique using algorithms were applied for lithological discrimination of different rock units.

RESULT

5.1. Band Ratio

Landsat ETM+ band ratio composite (7/1, 3/1, 5/7) is used in the present study and proved to be effective in lithological discrimination, the ratioshows clear and obvious contacts for main rock units. The study area is considered as a good representative for the arid regions.The serpentinites appears in a dark-blue color,metagabbro has blue color, fresh gabbro has greyish brown color, metavolcanics have a reddish violet color, metavolcanosedimenrty rocks have dark red color wherease schists have a mixture of the previous two colors. Granitoids also can be identified clearly in this ratio, where El-Sibai, Nusla and Um Shaddad granites have orange color, while Kadabora granite has pale orange to pale yellow color owing to the contact of dyke swarms, Biotite granites has dark orange to redish brown color,where as tonalite has more pinkish color and migmatites appear with pale red color (Fig. 4). This ratio has almost identified all the rock units in the study area and show clear obvious contacts between them which considered a very effective ratio to use for mapping, also can be used as aguide during field studies in the arid regions especially in the Arabian-Nubian Shield region.

Comparison between the previously published band ratios was carried out (Sultan et al., 1986, Sabins, 1999and Gad and Kusky, 2006) and the result obtained from the present study supports the conclusion about the useful of the newly adapted band ratio image. In Sultan's ratio (5/7, 5/1, 5/4 * 3/4RGB), the serpentinites appeared bright in color (red) owing to the band seven absorption by MgO– and OH– bearing minerals (Fig. 5), while in Sabin'sratio (3/5, 3/1, 5/7 RGB), the serpentinites appear in violet color (Fig. 6). In Gad and Kusky band ratio image (5/3, 5/1, 7/5RGB), the serpentinites appear in a dark-brown green color while the metavolcanics have a pinkish yellow color (Fig. 7), whereas in the band ratio image (7/5, 5/4, 3/1RGB) (Fig. 8) shows that the serpentinites can be distinguished by their dark brownish color and the associated metavolcanics are identified by their yellowish-green color.

5.2. Supervised Classification

Supervised classification technique is also used in the present study. Classification was done by using a region of interests and the spectral signatures.

5.2.1. Supervised Classification using Region of Interests (ROIs)

Regions of interest (ROIs) are portions of images, either selected graphically or selected by other means such as thre sholding. These regions can be irregularly-shaped and are used to extract statistics for classification. Regions of interests were selected carefully for every rock unit from different localities and were distributed well all over the scene. Selecting these regions were depending upon the field observation and the old maps. Two algorithms were used successfully to classify the images with this (ROIs).

Maximum Likelihood (ML): This classification assumes that the statistics for each class in each band were normally distributed and calculates the probability that a given pixel belongs to a specific class. Unless a probability threshold, all pixels were classified. Each pixel was assigned to the class that has the highest probability (that is, the maximum likelihood). If the highest probability is smaller than a threshold, we specify, the pixel remains unclassified.

ENVI implements maximum likelihood classification by calculating the following discriminate functions for each pixel in the image (Richards, 1999):

$$g_i(x) - \ln p(\omega_i) - \tfrac{1}{2} \ln |\Sigma_i| - \tfrac{1}{2}(x - m_i)^t \Sigma_i^{-1} (x - m_i)$$

Where: i = class; x = n-dimensional data (where n is the number of bands); p (ωi) = probability that class ωi occurs in the image and is assumed the same for all classes; |Σi| = determinant of the covariance matrix of the data in class ωi; Σi-1 = its inverse matrix; mi = mean vector

In the present study, maximum likelihoods were applied on the Landsat ETM+ bands in the study area using (ROIs) with overall accuracy 90.6% (Fig. 9).

Support Vector Machine (SVM): is a supervised classification method derived from statistical learning theory. It separates the classes with a decision surface that maximizes the marg in between the classes. The surface is often called the optimal hyperplane, and the data points closest to the hyperplane are called support vectors. The support vectors are the critical elements of the training set. We performed that classification to identify the class associated with each pixel. It yiels good classification results from complex and noisy data.SVM was applied to the Landsat ETM+ bands in the study area using (ROIs) with overall accuracy 90.04% (Fig. 10).

5.1.2. Supervised Classification using Spectral Signature

In the present study, supervised classification applied using the spectral signatures of rock unit. Three different algorithms were applied.

Spectral Angle Mapper (SAM): The SAM method produces a classified image based on the value specified for SAM Maximum Angle. Decreasing this threshold usually results in fewer matching pixels (better matches to the reference spectrum). Increasing this threshold may result in a more spatially coherent image; however, the overall pixel matches will not be as good as for the lower threshold. This technique was applied on the Landsat ETM+ bands (Fig. 11).

Minimum Distance (DM): This technique uses the mean vectors of each end-member and calculates the Euclidean distance from each unknown pixel to the mean. All pixels are classified to the nearest class unless a standard deviation or distance threshold is specified. This technique was applied on the Landsat ETM+ bands (Fig. 12).

Spectral Information Divergence (SID): The classification uses a divergence measure to match pixels to reference spectra. The smaller the divergence, the more likely the pixels are similar. Pixels with a measurement greater than the specified maximum divergence threshold are not classified. This technique was applied on the Landsat ETM+ bands (Fig. 13).

The results show that SID can characterize spectral similarity of variability more effective than SAM.

6. Conclusion

The enhancement techniques applied in the present study combined with the field observation and previous lithological mapping studies in the Wadi Um Gheig area, allow to distinguish between the different rock units and help to detect the contacts between them. Sultan et al. (1986) and other authors applied several band ratio images to the different rocks in the Eastern Desert of Egypt. Most of the authors tried to distinguish only one rock unit. Theywere exploring this unit not mapping all area. In contrast, the present authors used the same techniques compiled with new proposed ratio (7/1, 3/1, 5/7 RGB), it shows a pronounced ability in mapping rocks within the study area.Comparing with the previous published ratios, it can be noticed that the newly band ratio provide a great advantage than the previously published bands. Mapping by using the region of interest gave a better result in classification,as we depend on spectra from the spectral library found at software (future studies will take into concern taking spectra from rocks at field and make a spectrum library for the study area, detailed studies will be on unmixing of a pixel spectrum), Maximum likelihood classification showed 90.4% of overall accuracy that was done after field and petrographical studies.

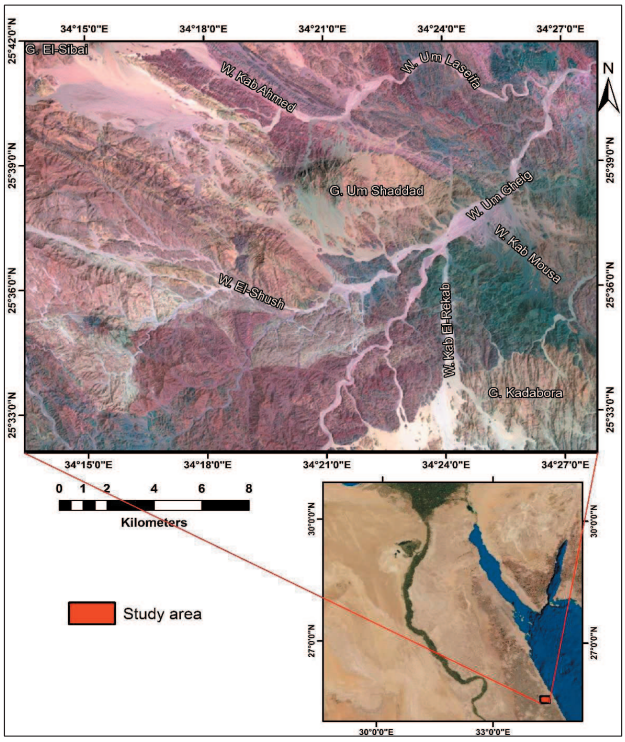

Fig. 1. Landsat Enhanced Thematic Mapper (ETM+) image (7, 4, 2) in RGB showing the location of the study area.

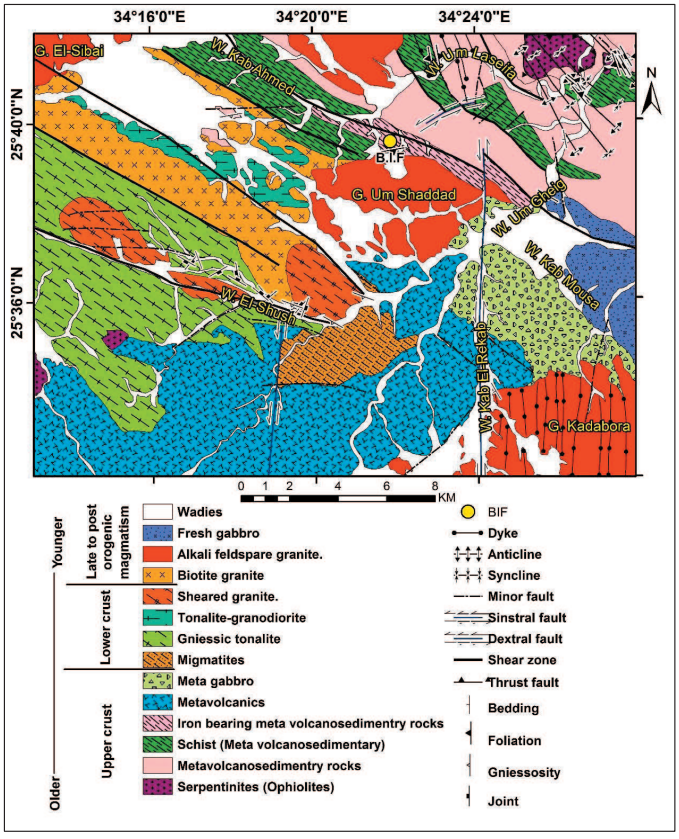

Fig. 2: Geologic map of Wadi Um Gheig area.

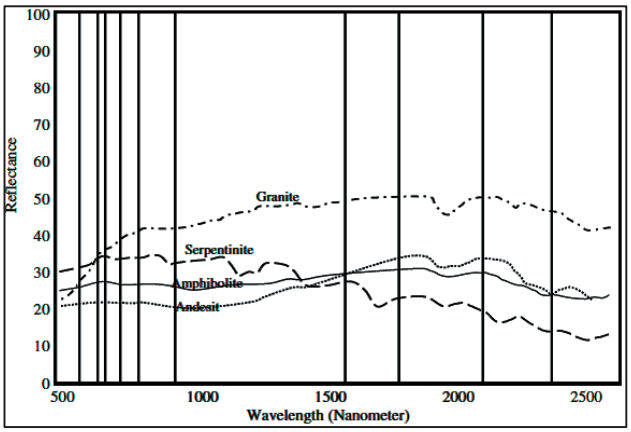

Fig. 3: Spectral reflectance of the serpentinites, granites and metavolcanics (andesite and amphibolites) for the Eastern Desert, Egypt (Frei and jutz, 1989).

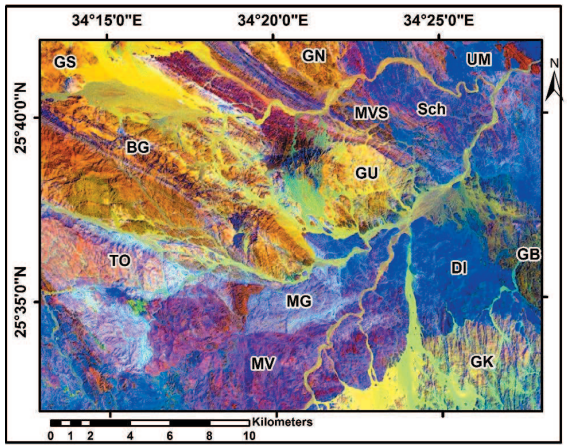

Fig. 4: Color ratio Landsat ETM+ bands (7/1, 3/1, 5/7 RGB) for the study area. (GS: El-Sibai ganite, GN: Nuslaganite, GU: Um Shaddadganite, GK: Kadabora granite, BG: biotite granite, TO: tonalite, MG: migmatites MV:metavolcanics, MVS: metavolcanosed imentary,Sch: schists, UM: ultramafic, DI: Meta gabbro and GB: Fresh Gabbro).

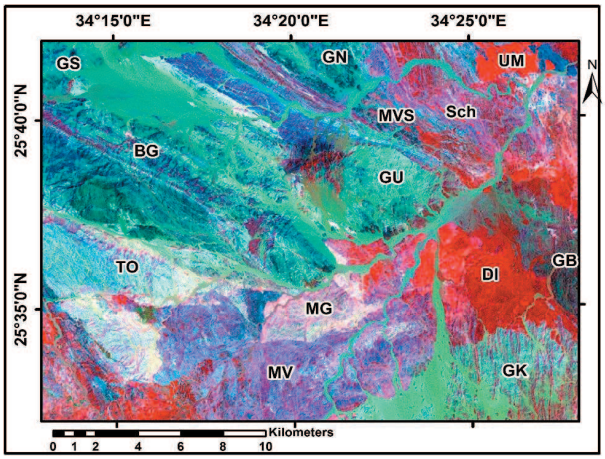

Fig. 5: Landsat RGB color ratio image (5/7, 5/1, 5/4 * 4/3, Sultan et al., 1986). Symbols as in Fig. 4.

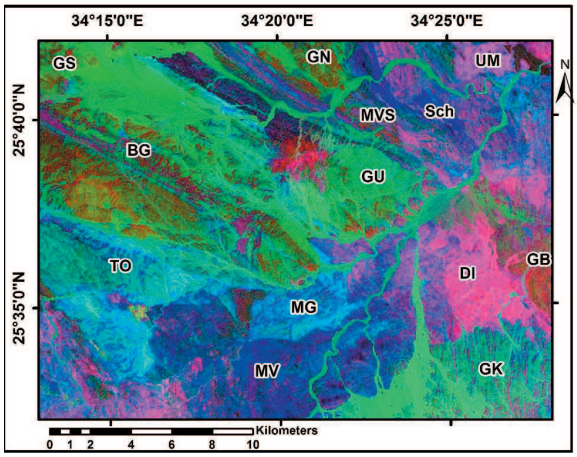

Fig. 6: Landsat RGB color ratio image (3/5, 3/1, 5/7,Sabins, 1999) for the study area.Symbols as in Fig. 4.

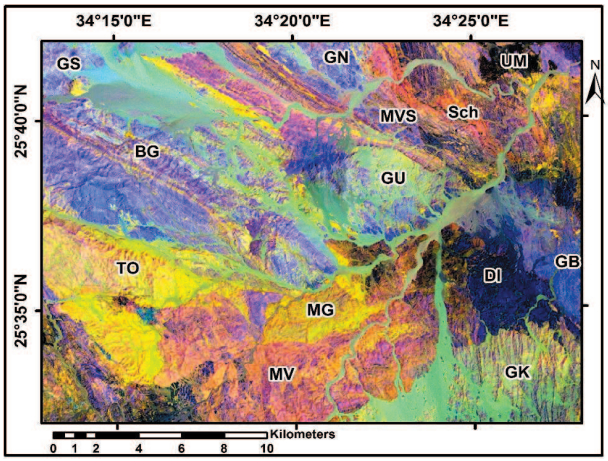

Fig. 7: Landsat RGB color ratio image (5/3, 5/1, 7/1Gad and Kusky, 2006)for the study area. Symbols as in Fig. 4.

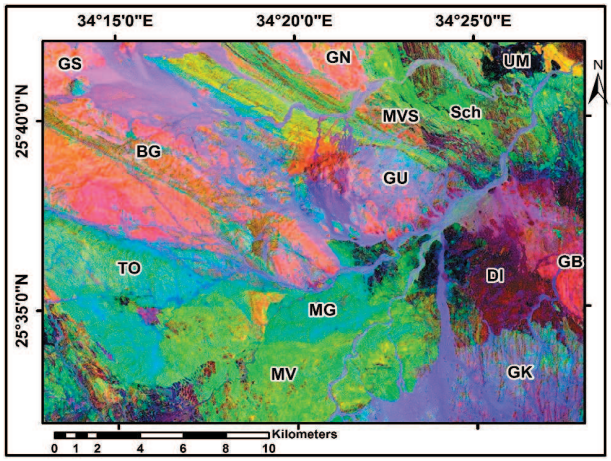

Fig. 8: Landsat RGB color ratio image (7/5, 5/4, 3/1Gad and Kusky, 2006)for the study area. Symbols as in Fig. 4.

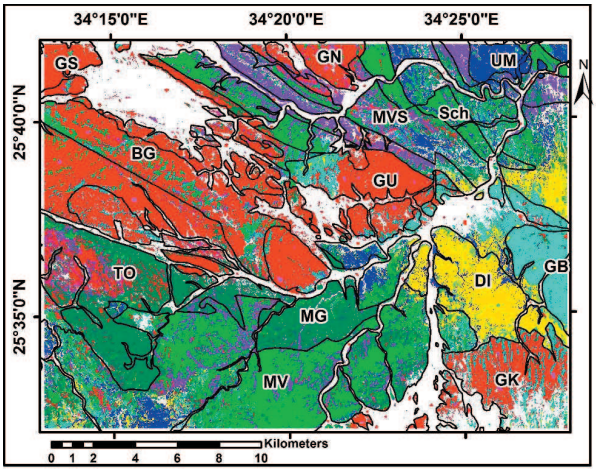

Fig. 9: Maximum likelihood classification using ROIs for the study area.Symbols as in Fig. 4.

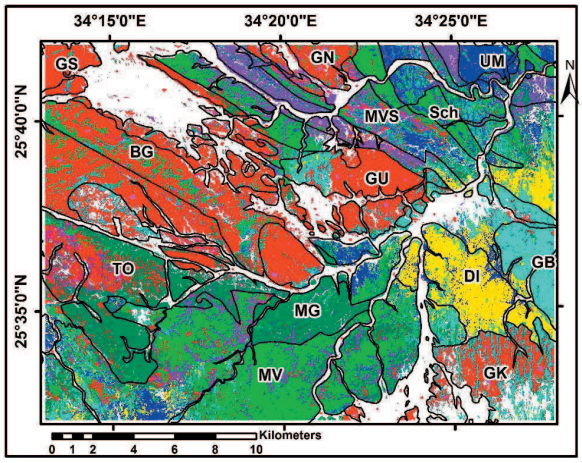

Fig. 10: Support vector machine classificatiousing ROIs for the study area.Symbols as in Fig. 4.

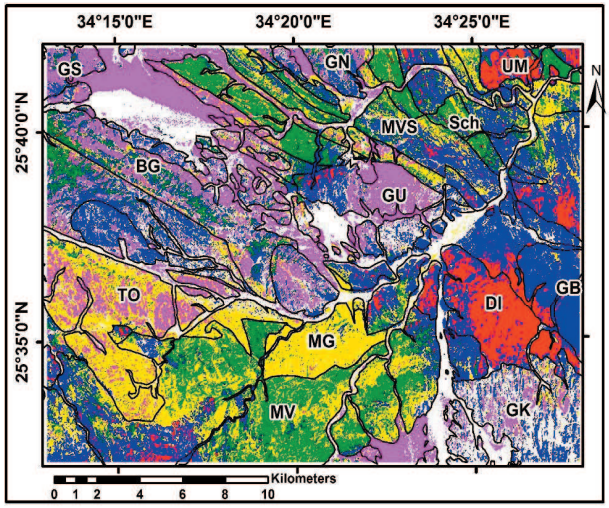

Fig. 11: Spectral angular mapper classification using spectral signatures for the study area.Symbols as in Fig. 4.

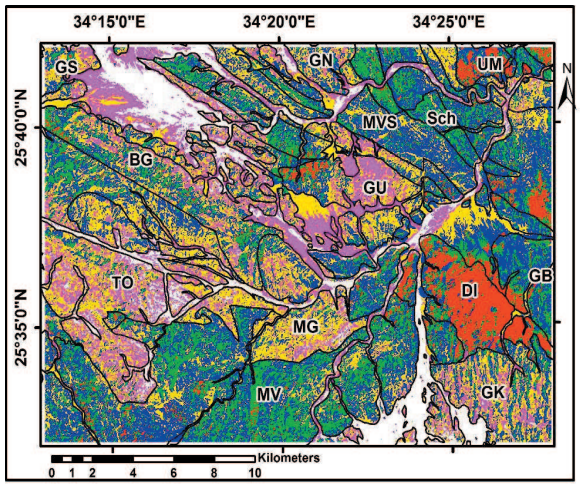

Fig. 12: Minimum distance classification using spectral signatures for the study area.Symbols as in Fig. 4.

REFERENCES

Abd El-Wahed, M.A., 2006. Structures related to transpretion in the Neoproterozoic cover nappe Southwest El-Sibai core complex, Central Eastern Desert, Egypt. Egyptian Journal of Geology, V.50, pp.227-263.

Abdeen, M.M., 2003. Tectonic history of the Pan-African orogeny in Um Gheig area, Central Eastern Desert, Egyptian Journal of Geology, V. 47, pp. 239–254.

Abdelsalam, M.G., Stern, R.J., 1999. Mineral exploration with satellit eremote sensing imagery: examples from Neoproterozoic Arabian Shield. Journal of African Earth Sciences 28, 4a.

Abrams, M.J., Brown, D., Lepley, L., Sadowski, R., 1983. Remote sensing for porphyry copper deposits in southern Arizona. Economic Geology 78, pp. 591–604.

Asran, M. H. A., 1991. Geology of Wadi Um Ghieg area, Eastern Desert of Egypt, Ph.D. dissetrainon,AssiutUniveristy, 276 p.

Blasband B., White, S., Brooijmans, P., De Boorder, H., and Visser, W., 2000, Late Proterozoic extensional collapse in the Arabian-Nubian Shield, Journal of the Geological Society, V. 157(3), pp. 615-628.

Bregar, M., A. Bauernhofer, K. Pelz, U. Kloetzli, H. Fritz & P. Neumayr, 2002. A late Neoproterozoic magmatic core complex in the Eastern Desert of Egypt: emplacement of granitoids in a wrench-tectonic setting, Precambrian Research, V. 118, pp. 59-82.

Crane, R. B., 1971. Processing techniques to reduce atmospheric and sensor variability in multi spectral scanner data. Proceed 7th. International Symposium on Remote Sensing of Environment, Ann Arbor, Vol.2, pp. 1345-1355.

Crippen, R. E., 1989. Selection of Landsat TM band and band-ratio combinationsto maximize lithologic information in color composite displays. In: Proceedings of the Seventh Thematic Conference on Remote Sensing for Exploration Geology,Vol. II, pp. 912–921.

Drury, S. A., 1987. Image interpretation in geology.1st. ed., 243 p.,(Allen&Unwin) London.

El Gaby, S., 1983. Architecture of the Egyptian basement complex. International Basement Tectonics Association, V. 5, p. 8.

El Ramly, M.F., Greiling, R., Rashwan, A.A., Rasmy, A.H., 1993. Geologic map of Wadi Hafafit area. Scale 1:100.000. Egyptian Geological Survey, p.68.

Fowler, A., Khamees, H., Dowidar, H., 2007. El Sibai gneissic complex, Central Eastern Desert, Egypt: folded nappes and syn-kinematic gneissic granitoid sheets not a core complex. Journal of African Earth Sciences, V. 49, pp.119–135.

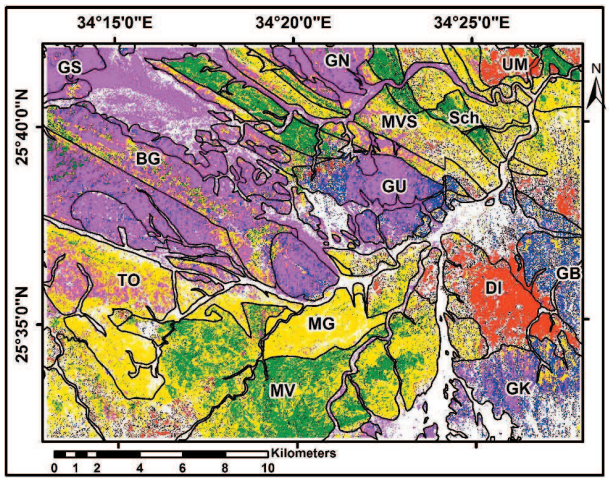

Fig. 13: Spectral information divergence classification using spectral signatures for the study area.Symbols as in Fig. 4.

Frei, M., Jutz, L., 1989. Use of Thematic Mapper data for the detection of gold bearing formations in the Eastern Desert of Egypt. In: Proceedings of the 7th thematic conference on remote sensing for ore exploration geology, Calgary, Canada, pp. 1157–1172.

Gad, S. and KUSKY, T., 2006. Lithological mapping in the Eastern Desert of Egypt, the Barramiya area, using Landsat thematic mapper (TM). Journal of African Earth Sciences, 44(2): 196-202.

Habib, M.E., A.A. Ahmed and O.M. El Nady, 1985: Tectonic evolution of the Meatiq infrastructure, Central Eastern Desert, Egypt. Tectonics American Geophysical Union, V4, 7, pp. 613- 627.

Ibrahim, S. and J. Cosgrove, 2001: Structural and tectonic evolution of the Umm Gheig/El-Shush region, central Eastern Desert of Egypt, Journal of African Earth Science, V. 33, 2, pp.199-209.

Johnson, P. R., Andresen, A., Collins, A. S., Fowler, A. R., Fritz, H., Ghebreab, W., Kusky, T., Stern, R. J., 2011. Late Cryogenian-Ediacaran history of the Arabian–Nubian Shield: A review of depositional, plutonic, structural, and tectonic events in the closing stages of the northern East African Orogen. Journal of African Earth Sciences, V. 61, pp.167-232.

Kamal El Din, G.M., 1991: Geochemistry and tectonic significance of the Pan-African El Sibai window, Central Eastern Desert, Egypt, Ph.D. dissertation, Heidelberg University, Germany, 114 p.

Kaufmann, H., 1988. Mineral exploration along the Aqaba—Leventstructure by use of Landsat TM data; concepts, processing, and results.International Journal of Remote Sensing 9, 1639–1658.

Khudeir, A.A., S. El-Gaby, G. M. Kamal El-Din, A.M.H. Asran and R.O. Greiling, 1995: The pre-Pan-African deformed granite cycle of the Gabal El-Sibai swell, Eastern Desert, Egypt.- Journal of African Earth Sciences, V. 21, pp.395-406.

Kusky, T.M. and Matsah, M.I., 2003. Neoproterozoic dextral faulting on the Najd Fault System, Saudi Arabia, preceded sinistral faulting and escape tectonics related to closure of the Mozambique Ocean. Geological Society, London, Special Publication, 206: 327-361.

Kusky, T.M. and Ramadan, T.M., 2002. Structural controls on Neoproterozoic mineralization in the South Eastern Desert, Egypt: An integrated field, Landsat TM and SIR C/X approach. Journal of African Earth Sciences, 35(1): 107-121.

Ragab, A.I., B. El-Kaliobi and Z. El-Alfy, 1993: Petrotectonic assemblages and crustal evolution of the area north of Abu El-Tiyur, central Eastern Desert, Egypt. Middle East Research Center,Ain Shams University, earth Science Series, Vol. 7, pp. 1-16.

Richards, J.A., 1999, Remote Sensing Digital Image Analysis, Springer-Verlag, Berlin, 240 p.

Sabins, F.F., 1999. Remote Sensing for mineral exploration. Ore Geology Review, 14(3-4): 157-183.

Stern, R.J. and Hedge, C.E., 1985. Geochronologic and isotopic constraints on Late Precambrian crustal evolution in the Eastern Desert of Egypt. American Journal of Science, 285: 97-127.

Stern, R.J., 1994. Arc assembly and continental collision in the Neoproterozoic East African Orogen: implications for the consolidation of Gondwanaland. Annual Review of Earth and Planetary Sciences, 22: 319-351.

Sultan, M., Arvidson, R.E., Sturchio, N.C., 1986. Mapping of serpentinites in the Eastern Desert of Egypt using Landsat Thematic Mapper data. Geology 14, 995–999.

Youssef, A. M., Zaghloul, E. A., Moussa, M. F. and Mahdi, A. M., 2009. Lithological mapping using landsat enhanced thematic mapper in the Central Eastern Desert, Egypt: case study: area surround GabalAl Haded. The Egyptian Journal of Remote sensing and space science, v.12, pp. 87-10.